ISSN 0554-6397
UDK: 004.032.26
Original Scientific Paper
Received: 1st April 2025.

Nikola Anđelić
E-mail: nikola.andjelic@riteh.uniri.hr
University of Rijeka, Faculty of Engineering, Vukovarska 58, 51000 Rijeka, Croatia
Sandi Baressi Šegota
E-mail: sandi.baressi.segota@unipu.hr
Juraj Dobrila University of Pula, Faculty of Informatics, Alda Negrija 6, 52100 Pula, Croatia
Igor Poljak
E-mail: ipoljak1@unizd.hr
University of Zadar, Maritime Department, Mihovila Pavlinovića 1, 23000 Zadar, Croatia
Vedran Mrzljak
E-mail: vedran.mrzljak@riteh.uniri.hr
University of Rijeka, Faculty of Engineering, Vukovarska 58, 51000 Rijeka, Croatia

The Ambient Temperature Influence on the CO_2 Low-power Marine Waste Heat Recovery Plant at Several Loads

Abstract

This paper presents an exergy analysis of a marine CO_2 low-power waste heat recovery plant and its individual components under varying ambient temperatures and three load conditions. At nominal load, the analyzed power plant produces only 146.95 kW of useful power. An increase in ambient temperature results in higher exergy destruction and a simultaneous decrease in exergy efficiency for both the whole plant and each plant component. Considering all loads and ambient temperatures, all turbomachines from the analyzed plant (turbine, main compressor, and auxiliary compressor) exhibit high exergy efficiencies (exceeding 90%). The exergy efficiencies of the turbomachines are higher in comparison to any heat exchanger from the observed power plant. Within the analyzed ambient temperature range, the cumulative change in exergy efficiency of each turbomachine at any load is approximately 1% or less, while the cumulative change for each heat exchanger at any load is approximately 4% or higher. This indicates that turbomachinery performance is considerably less sensitive to ambient temperature variations than that of heat exchangers. Among all plant components, the cooler demonstrates the lowest exergy efficiencies, not exceeding 38%. Furthermore, its exergy efficiency is several times more sensitive to ambient temperature changes compared to the other plant components. Under optimal operating conditions, the overall plant exergy efficiency reaches approximately 34%. This relatively low exergy efficiency of the whole plant can be attributed to the use of only a single waste heat flow from a marine low-speed diesel engine (combustion gases). For such CO_2 waste heat recovery plants, it is recommended to use various waste heat flows from the internal combustion engine at different temperature levels – in that situation much higher exergy efficiencies of the whole plant can be achieved.

Keywords: the ambient temperature change, exergy analysis, CO_2 waste heat recovery plant, various plant loads

1. Introduction

In the marine sector, diesel engines currently dominate as the dominant sources of mechanical power [1, 2]. Due to their widespread application in the marine sector, diesel engines are often analyzed and optimized in various directions with the primary objective of improving overall performance [3-5]. Various kinds of numerical simulations enable accurate and precise monitoring of diesel engine operating parameters, offering a more cost-effective and practical alternative to performing measurements [6-8]. Significant research efforts are focused on reducing fuel consumption and various harmful emissions from marine diesel engines, particularly in response to increasingly stringent environmental regulations [9-12].

Low-speed two stroke diesel (or dual fuel) engines are the most important main propulsors at the moment [13, 14]. During their operation, several heat sources are generated that can be effectively utilized instead of being discharged into the environment [15, 16]. For example, cooling water or combustion gases at the engine outlet, and compressed air prior to entering the engine cylinders contain substantial heat flows and relatively high temperatures. These energy sources can be exploited in various additional waste heat recovery plants [17, 18]. Such plants can serve various purposes, including additional mechanical power generation [19, 20]. Waste heat recovery plants can be highly beneficial for increasing the overall efficiency of the system (diesel engine + waste heat recovery plant) [21, 22].

A review of literature indicates that in the marine sector researchers have frequently proposed waste heat recovery plants based on closed-cycle gas turbines using CO_2 as the main working fluid [23-25]. These systems typically include at least two heat exchangers (a heater and a cooler), as well as a turbocompressor and a turbine, to ensure proper operation [26, 27]. In many cases, additional heat exchangers or system modifications are incorporated to maximize heat utilization and improve overall plant efficiency [28-30].

In this paper, an exergy analysis is conducted on a marine low-power closed-cycle gas turbine waste heat recovery plant operating with CO_2 as the working fluid, considering variations in ambient temperature. The primary heat source for the analyzed plant consists of combustion gases from a marine low-speed diesel engine. The plant is examined (from an exergy perspective) under three engine load conditions, with ambient temperature variation applied in each case. The analysis and ambient temperature variation involve each component of the observed waste heat recovery plant as well as the whole plant. For each component and whole plant at each load condition, changes in exergy parameters resulting from ambient temperature variation are presented, and the component most sensitive to ambient temperature changes is detected. The underlying reasons for the observed sensitivity of each component are analyzed and discussed. The exergy efficiency of the plant analyzed is compared with that of a similar waste heat recovery plant utilizing multiple heat sources from the diesel engine, in contrast to the present system, which relies solely on exhaust gases as its heat source.

2. Specifications and operating characteristics of the CO_2 low-power marine waste heat recovery plant

General scheme of the analyzed closed-cycle gas turbine CO_2 low-power marine waste heat recovery plant, including operating points (from 1 to 16) required for the exergy analysis of both the overall plant and its individual components is shown in Figure 1. As illustrated in Figure 1, the system consists of four heat exchangers, one gas turbine, and two turbocompressors.

The main heater is the heat exchanger in which the CO_2 is heated to its maximum temperature. The CO_2 temperature at the main heater outlet depends on the combustion gases inlet parameters. In the main heater, heat is transferred from the combustion gases to the CO_2 through pipe walls. At all considered load conditions, the combustion gases are supplied to the main heater from the 6EX340EF marine low-speed diesel engine [31]. CO_2 at the highest temperature in the cycle (operating point 1, Figure 1) enters the turbine where it expands. Turbine produces mechanical power; a portion of cumulatively produced mechanical power by the turbine is used for the main and auxiliary compressor drive, while the remaining portion of the produced mechanical power (useful power) is used to drive the electrical generator.

After expansion in the turbine, the CO_2 flows to the high-temperature recuperator. High temperature recuperator is a CO_2-CO_2 heat exchanger in which the hotter CO_2 stream transfers heat to a colder CO_2 stream through pipe walls. The high temperature recuperator actually increases the CO_2 temperature before it enters the main heater (operating point 12, Figure 1), thereby utilizing waste heat from the turbine and improving overall plant efficiency [32]. Directly after the high temperature recuperator, the CO_2 enters the low temperature recuperator, another CO_2-CO_2 heat exchanger. The same heat exchange process occurs in this component as in the high temperature recuperator, but at lower CO_2 temperature levels.

After leaving the low temperature recuperator (operating point 4, Figure 1), the CO_2 mass flow rate is divided into two flow streams. One flow stream is directed to the auxiliary compressor, while the other flow stream is sent to the cooler. At all considered load conditions, the CO_2 mass flow rate entering the auxiliary compressor is significantly lower than the CO_2 mass flow rate directed to the cooler. The auxiliary compressor increases the CO_2 pressure (as well as temperature) and returns the compressed flow to the main flow stream between the high- and low-temperature recuperators (operating point 6, Figure 1). The CO_2 mass flow rate directed to the cooler is cooled to the main compressor inlet temperature (operating point 8, Figure 1). Water is used as the cooling medium in the cooler, with heat transferred from the higher-temperature CO_2 to the lower-temperature water. The cooled CO_2 then enters the main compressor, while the heated water (operating point 14, Figure 1) exits the observed plant. Finally, the main compressor raises the CO_2 pressure to the highest level in the plant. This pressure must be sufficient to enable the CO_2 to pass through both low- and high-temperature recuperators and enter the main heater.

According to the literature [31], the plant shown in Figure 1 is designed to operate with CO_2 as the main working fluid. One potential direction for future research, alongside optimization and performance improvement studies using various numerical models and techniques [33-35], is the analysis of alternative gas usage instead of CO_2. Various other gases, such as nitrogen, helium, or argon, could potentially be used in this plant, so it would be interesting to see the whole plant and each component's performance when the other gases are used [36]. However, due to different thermodynamic properties of other gases in comparison to CO_2, significant changes in operating parameters at each operating point from Figure 1 would be expected.

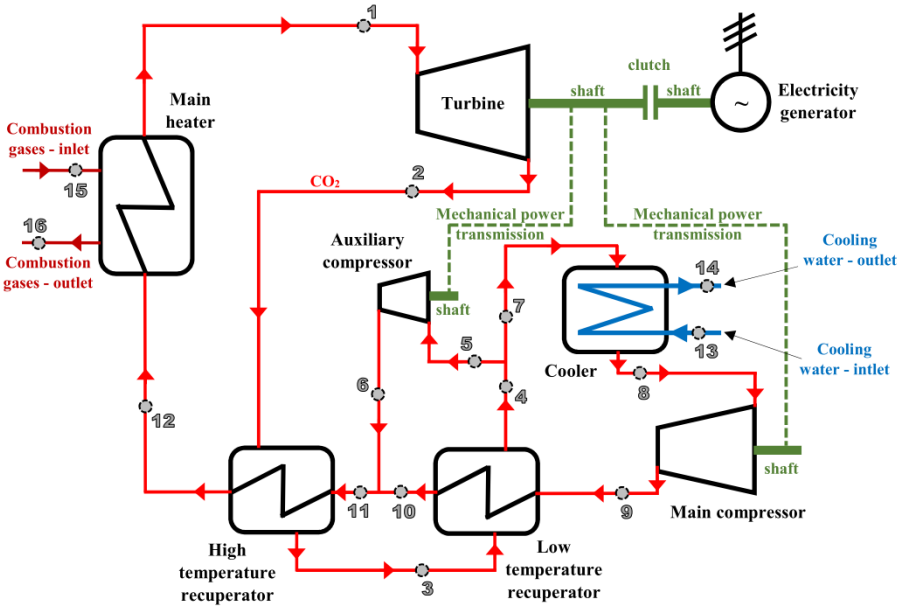

Figure 1. General scheme of the analyzed CO_2 low-power marine waste heat recovery plant

Nowadays, marine waste heat recovery plants based on closed-cycle gas turbines, such as the plant analyzed in this paper, predominantly use CO_2 as the working fluid. The widespread application of CO_2 in these systems is primarily due to its favorable thermodynamic properties, relatively low cost, and global availability. Compared to other gases, CO_2 exhibits a significantly smaller temperature increase during compression, which facilitates effective waste heat utilization at various temperature levels [24]. The analysis performed in this paper also demonstrates that a substantial CO_2 pressure increase in the main compressor results in only a moderate rise in CO_2 temperature, which cannot be achieved with most alternative gases considered for

this type of system. For this reason, the selection of the working fluid is a critical decision at the design stage of any closed-cycle gas turbine. In the real exploitation conditions, changing the working fluid can be highly challenging, as it may require substantial system modifications or may prove technically unfeasible and economically unjustifiable.

3. Exergy analysis and the ambient temperature variation

In contrast to energy analysis, which is based on the first law of thermodynamics and does not account for ambient conditions [37, 38], exergy analysis is founded on the second law of thermodynamics and explicitly incorporates ambient parameters (ambient pressure and temperature) under which the analyzed plant or component operates [39, 40]. Only through exergy analysis can the influence of changes in ambient temperature or pressure on system efficiencies and irreversibilities be properly evaluated [41, 42].

Both energy and exergy analyses can be regarded as "black box" methods, since knowledge of the internal structure of the analyzed component is not required [43]. The essential inputs for such analyses are fluid, power, and heat flows only (inlet and outlet flows related to each observed component) [44].

Many researchers prefer exergy analysis over energy analysis when evaluating various plants and/or components because it provides more relevant parameters [45, 46]. Furthermore, exergy analysis often serves as a foundation for further, more advanced studies [47-50].

3.1. Base exergy analysis equations, balances, and principles

During the exergy analysis of any plant or component, some base equations, balances, and principles must always be satisfied [51, 52]. The base exergy balance equation for any plant or component is [53]:

$$\dot{X}_{\mathrm{H}} - P = \sum \dot{E}x_{\mathrm{OUT}} - \sum \dot{E}x_{\mathrm{IN}} + \dot{E}x_{\mathrm{DES}}, \tag{1}$$

where P is mechanical power, index IN is related to the inlet flow stream, index OUT is related to the outlet flow stream, while DES is related to the exergy destruction.

$\dot{E}x$ in Eq. 1 is a total fluid exergy flow, defined by an equation [54]:

$$\dot{E}x = \dot{m} \cdot \psi, \tag{2}$$

where $\dot{m}$ is fluid mass flow rate and ψ is fluid specific exergy. Fluid specific exergy (ψ) is defined by an equation [55]:

$$\psi = (h - h_0) - T_0 \cdot (s - s_0). \tag{3}$$

In Eq. 3, h is fluid specific enthalpy, s is fluid specific entropy, T is a temperature, and index 0 is related to the base ambient state. The base ambient state in exergy analysis can be changed (change of the base ambient temperature T_0 and possible change in the base ambient pressure) results in a change in fluid specific enthalpy (h_0) and fluid specific entropy (s_0) at the base ambient state, which results in a change in fluid specific exergy. Such change in fluid specific exergy (of each fluid stream) finally results in a notable change in the observed component or entire plant exergy parameters. Eq. 3 clearly shows that the change in the base ambient temperature (T_0) has a direct and much more significant influence on the fluid specific exergy in comparison to the change in the base ambient pressure.

The last undefined variable from Eq. 1 is an exergy heat transfer at the temperature T ($\dot{X}_{\mathrm{H}}$), which is defined by the equation [56]:

$$\dot{X}_{\mathrm{H}} = \sum(1 - \frac{T_0}{T}) \cdot \dot{Q}, \tag{4}$$

where $\dot{Q}$ is energy heat transfer. Again, as Eq. 3, Eq. 4 shows a direct influence of the base ambient temperature (T_0) on the exergy heat transfer.

Fluid mass flow rate balance of any plant or component is [57]:

$$\sum \dot{m}_{\mathrm{IN}} = \sum \dot{m}_{\mathrm{OUT}}, \tag{5}$$

while the general exergy efficiency equation of any plant or component can be expressed as [58]:

$$\eta_{\mathrm{EX}} = \frac{\mathrm{CUMULATIVE\ EXERGY\ OUTLET}}{\mathrm{CUMULATIVE\ EXERGY\ INLET}}. \tag{6}$$

It must be highlighted that Eq. 6 can have many different shapes and forms (Eq. 6 is just a general and overall presentation), which depends on the plant or component operation characteristics.

3.2. Equations for the exergy analysis and the ambient temperature variation of the analyzed CO_2 low-power marine waste heat recovery plant and its components

The exergy analysis equations for the overall plant and each individual component are formulated in accordance with recommendations from the available literature [59-61]. The same set of equations presented in this subsection is applied during the ambient temperature variation; only the specific exergy of each fluid stream changes as a result of varying ambient conditions.. Likewise, all the presented equations remain unchanged for different plant loads, while variations occur solely in the operating parameters of the working fluids. For each component and for the entire plant, equations are defined for the calculation of exergy inflow, exergy outflow, exergy destruction,

and exergy efficiency [62]. The symbols and indexes used in the equations presented in this subsection correspond to the operating points shown in Figure 1.

The analyzed CO_2 low-power marine waste heat recovery plant includes one mechanical power producer (the turbine) and two mechanical power consumers (the main compressor and the auxiliary compressor). The exergy analysis of each mechanical power producer, consumer, as well as the overall plant requires calculation of produced, consumed, and useful mechanical power. Each mentioned mechanical power can be calculated according to the guidelines from [63, 64].

Cumulative mechanical power produced by the turbine is:

$$P_{\text{Turbine}} = \dot{m}_1 \cdot (h_1 - h_2). \tag{7}$$

Mechanical power consumed by the main and auxiliary compressor is:

$$P_{\text{Main compressor}} = \dot{m}_8 \cdot (h_9 - h_8), \tag{8}$$

$$P_{\text{Auxiliary compressor}} = \dot{m}_5 \cdot (h_6 - h_5). \tag{9}$$

Useful mechanical power is the difference between cumulative mechanical power produced by the turbine and the mechanical power consumed by both compressors (main and auxiliary). Useful mechanical power in the observed plant is used for the electricity generator drive (Figure 1). Useful mechanical power of the analyzed CO_2 low-power marine waste heat recovery plant is:

$$P_{\text{Useful}} = P_{\text{Turbine}} - (P_{\text{Main compressor}} + P_{\text{Auxiliary compressor}}). \tag{10}$$

Exergy analysis equations of mechanical power producer (turbine) and mechanical power consumers (main compressor and auxiliary compressor) in the observed CO_2 low-power marine waste heat recovery plant are formulated according to [65, 66] and presented in Table 1.

Table 1. Exergy analysis equations of the turbine and both compressors (main and auxiliary) from the observed CO_2 low-power marine waste heat recovery plant

Component	Exergy inflow	Eq.	Exergy outflow	Eq.
Turbine	$\dot{E}x_{\mathrm{IN,Turbine}} = \dot{E}x_1$	(11)	$\dot{E}x_{\mathrm{OUT,Turbine}} = \dot{E}x_2 + P_{\mathrm{Turbine}}$	(14)
Main compressor	$\dot{E}x_{\mathrm{IN,Main\ compressor}} = \dot{E}x_8 + P_{\mathrm{Main\ compressor}}$	(12)	$\dot{E}x_{\mathrm{OUT,Main\ compressor}} = \dot{E}x_9$	(15)
Auxiliary compressor	$\dot{E}x_{\mathrm{IN,Auxiliary\ compressor}} = \dot{E}x_5 + P_{\mathrm{Auxiliary\ compressor}}$	(13)	$\dot{E}x_{\mathrm{OUT,Auxiliary\ compressor}} = \dot{E}x_6$	(16)
Component	**Exergy destruction**	**Eq.**	**Exergy efficiency**	**Eq.**
Turbine	$\dot{E}x_{\mathrm{DES,Turbine}} = \dot{E}x_{\mathrm{IN,Turbine}} - \dot{E}x_{\mathrm{OUT,Turbine}}$	(17)	$\eta_{\mathrm{EX,Turbine}} = \frac{P_{\mathrm{Turbine}}}{\dot{E}x_1 - \dot{E}x_2}$	(20)
Main compressor	$\dot{E}x_{\mathrm{DES,Main\ compressor}} = \dot{E}x_{\mathrm{IN,Main\ compressor}} - \dot{E}x_{\mathrm{OUT,Main\ compressor}}$	(18)	$\eta_{\mathrm{EX,Main\ compressor}} = \frac{\dot{E}x_9 - \dot{E}x_8}{P_{\mathrm{Main\ compressor}}}$	(21)
Auxiliary compressor	$\dot{E}x_{\mathrm{DES,Auxiliary\ compressor}} = \dot{E}x_{\mathrm{IN,Auxiliary\ compressor}} - \dot{E}x_{\mathrm{OUT,Auxiliary\ compressor}}$	(19)	$\eta_{\mathrm{EX,Auxiliary\ compressor}} = \frac{\dot{E}x_6 - \dot{E}x_5}{P_{\mathrm{Auxiliary\ compressor}}}$	(22)

Exergy analysis equations of all heat exchangers (high-temperature recuperator, low-temperature recuperator, main heater, and cooler) in the observed CO_2 low-power marine waste heat recovery plant are formulated according to [67, 68] and presented in Table 2.

Table 2. Exergy analysis equations of all heat exchangers from the observed CO_2 low-power marine waste heat recovery plant

Component	Exergy inflow	Eq.	Exergy outflow	Eq.
High-temperature recuperator (HTR)	$\dot{E}x_{\mathrm{IN,HTR}} = \dot{E}x_2 - \dot{E}x_3$	(23)	$\dot{E}x_{\mathrm{OUT,HTR}} = \dot{E}x_{12} - \dot{E}x_{11}$	(27)
Low-temperature recuperator (LTR)	$\dot{E}x_{\mathrm{IN,LTR}} = \dot{E}x_3 - \dot{E}x_4$	(24)	$\dot{E}x_{\mathrm{OUT,LTR}} = \dot{E}x_{10} - \dot{E}x_9$	(28)
Main heater	$\dot{E}x_{\mathrm{IN,Main\ heater}} = \dot{E}x_{15} - \dot{E}x_{16}$	(25)	$\dot{E}x_{\mathrm{OUT,Main\ heater}} = \dot{E}x_1 - \dot{E}x_{12}$	(29)
Cooler	$\dot{E}x_{\mathrm{IN,Cooler}} = \dot{E}x_7 - \dot{E}x_8$	(26)	$\dot{E}x_{\mathrm{OUT,Cooler}} = \dot{E}x_{14} - \dot{E}x_{13}$	(30)
Component	**Exergy destruction**	**Eq.**	**Exergy efficiency**	**Eq.**
High-temperature recuperator (HTR)	$\dot{E}x_{\mathrm{DES,HTR}} = \dot{E}x_{\mathrm{IN,HTR}} - \dot{E}x_{\mathrm{OUT,HTR}}$	(31)	$\eta_{\mathrm{EX,HTR}} = \frac{\dot{E}x_{\mathrm{OUT,HTR}}}{\dot{E}x_{\mathrm{IN,HTR}}}$	(35)

Low-temperature recuperator (LTR)	$\dot{E}x_{\mathrm{DES,LTR}} = \dot{E}x_{\mathrm{IN,LTR}} - \dot{E}x_{\mathrm{OUT,LTR}}$	(32)	$\eta_{\mathrm{EX,LTR}} = \frac{\dot{E}x_{\mathrm{OUT,LTR}}}{\dot{E}x_{\mathrm{IN,LTR}}}$	(36)
Main heater	$\dot{E}x_{\mathrm{DES,Main\ heater}} = \dot{E}x_{\mathrm{IN,Main\ heater}} - \dot{E}x_{\mathrm{OUT,Main\ heater}}$	(33)	$\eta_{\mathrm{EX,Main\ heater}} = \frac{\dot{E}x_{\mathrm{OUT,Main\ heater}}}{\dot{E}x_{\mathrm{IN,Main\ heater}}}$	(37)
Cooler	$\dot{E}x_{\mathrm{DES,Cooler}} = \dot{E}x_{\mathrm{IN,Cooler}} - \dot{E}x_{\mathrm{OUT,Cooler}}$	(34)	$\eta_{\mathrm{EX,Cooler}} = \frac{\dot{E}x_{\mathrm{OUT,Cooler}}}{\dot{E}x_{\mathrm{IN,Cooler}}}$	(38)

Exergy analysis equations for the overall observed CO_2 low-power marine waste heat recovery plant are defined according to [24, 69] and presented in Table 3.

Table 3. Exergy analysis equations of the whole CO_2 low-power waste heat recovery plant

/	**Whole plant**	**Eq.**
Exergy inflow	$\dot{E}x_{\mathrm{IN,Whole\ plant}} = \dot{E}x_{15} + \dot{E}x_{13}$	(39)
Exergy outflow	$\dot{E}x_{\mathrm{OUT,Whole\ plant}} = \dot{E}x_{14} + \dot{E}x_{16} + P_{\mathrm{Useful}}$	(40)
Exergy destruction	$\dot{E}x_{\mathrm{DES,Whole\ plant}} = \dot{E}x_{\mathrm{IN,Whole\ plant}} - \dot{E}x_{\mathrm{OUT,Whole\ plant}}$	(41)
Exergy efficiency	$\eta_{\mathrm{EX,Whole\ plant}} = \frac{P_{\mathrm{Useful}}}{\dot{E}x_{15} + \dot{E}x_{13} - \dot{E}x_{14} - \dot{E}x_{16}}$	(42)

4. Operating parameters required for the CO_2 low-power marine waste heat recovery plant and its components analysis at various loads

The exergy analysis and ambient temperature variation of the whole CO_2 low-power marine waste heat recovery plant and its components, at each considered load, are based on three base operating parameters for every operating point in Figure 1: fluid pressure, temperature, and mass flow rate.

Three load conditions are analyzed for the CO_2 low-power marine waste heat recovery plant and its components: nominal load (LOAD 100%) and two partial loads (LOAD 45% and LOAD 20%). The operating parameters for each plant operating point at LOAD 100% are presented in Table 4, while those at LOAD 45% and LOAD 20% are given in Tables 5 and 6, respectively. The base operating parameters for each operating point of the observed plant and load condition are obtained from the literature [31]. At each operating point, fluid pressure and temperature are used for the calculation of fluid specific enthalpy and fluid specific entropy by using NIST-REFPROP 9.0 software [70], while fluid specific exergy for each operating point at each load is calculated by using Eq. 3.

In addition to CO_2, two other working fluids are present in the observed plant: water in the cooler and combustion gases in the main heater. The base operating parameters of these fluids are also taken from the literature [31].

In any exergy analysis, a reference ambient state must be defined. This reference state is determined based on the expected ambient parameters under which the observed plant or component operates [71, 72]. In this analysis, the base ambient state is defined by an ambient temperature of 5 °C and an ambient pressure of 1 bar. Ambient pressure variation is not considered in this analysis, as pressure fluctuations under real exploitation conditions are relatively small and have a negligible effect on the exergy parameters of the observed plant and plant components.

Table 4. Power plant parameters in each operating point – LOAD 100%

O. P. *	Fluid	Temperature (°C)	Pressure (bar)	Mass flow rate (kg/s)	Specific enthalpy (kJ/kg)	Specific entropy (kJ/kg·K)	Specific exergy (kJ/kg) **
1	CO_2	220.00	194.50	8.300	626.56	2.1107	296.13
2	CO_2	150.73	92.80	8.300	576.46	2.1239	242.36
3	CO_2	130.32	91.90	8.300	551.47	2.0651	233.74
4	CO_2	97.55	91.50	8.300	507.41	1.9517	221.20
5	CO_2	97.55	91.50	2.075	507.41	1.9517	221.20
6	CO_2	170.28	194.85	2.075	556.98	1.9616	268.04
7	CO_2	97.55	91.50	6.225	507.41	1.9517	221.20
8	CO_2	45.00	90.90	6.225	386.97	1.5963	199.63
9	CO_2	93.58	195.05	6.225	413.64	1.6036	224.28
10	CO_2	120.32	194.85	6.225	472.80	1.7596	240.04
11	CO_2	129.93	194.85	8.300	491.00	1.8053	245.52
12	CO_2	144.16	194.55	8.300	516.00	1.8665	253.50
13	water	20.00	3.00	15.492	84.19	0.2964	1.84
14	water	31.00	2.90	15.492	130.17	0.4504	4.98
15	combustion gasses	249.00	3.20	10.600	652.16	4.1192	163.07
16	combustion gasses	160.25	2.92	10.600	561.03	3.9542	117.82

** O. P. = Operating Point (in accordance with Figure 1)*
*** At ambient temperature of 5 °C and ambient pressure of 1 bar*

Table 5. Power plant parameters in each operating point – LOAD 45%

O. P. *	Fluid	Temperature (°C)	Pressure (bar)	Mass flow rate (kg/s)	Specific enthalpy (kJ/kg)	Specific entropy (kJ/kg·K)	Specific exergy (kJ/kg) **
1	CO_2	206.99	194.50	4.600	609.10	2.0749	288.65
2	CO_2	139.55	92.80	4.600	562.62	2.0908	237.72
3	CO_2	137.48	91.90	4.600	560.52	2.0873	236.6
4	CO_2	95.12	91.50	4.600	503.84	1.9421	220.32
5	CO_2	95.12	91.50	1.288	503.84	1.9421	220.32
6	CO_2	168.39	194.85	1.288	554.15	1.9552	266.99
7	CO_2	95.12	91.50	3.312	503.84	1.9421	220.32
8	CO_2	44.00	90.90	3.312	380.05	1.5745	198.77
9	CO_2	90.36	195.05	3.312	405.6	1.5815	222.36
10	CO_2	124.72	194.85	3.312	481.30	1.7811	242.56
11	CO_2	135.34	194.85	4.600	500.71	1.8292	248.58
12	CO_2	137.17	194.55	4.600	504.07	1.8377	249.59
13	water	20.00	3.00	8.472	84.19	0.2964	1.84
14	water	31.00	2.90	8.472	130.17	0.4504	4.98
15	combustion gasses	236.99	1.30	5.900	639.83	4.3541	85.42
16	combustion gasses	152.83	1.18	5.900	553.63	4.1972	42.83

** O. P. = Operating Point (in accordance with Figure 1)*
*** At ambient temperature of 5 °C and ambient pressure of 1 bar*

Table 6. Power plant parameters in each operating point – LOAD 20%

O. P. *	Fluid	Temperature (°C)	Pressure (bar)	Mass flow rate (kg/s)	Specific enthalpy (kJ/kg)	Specific entropy (kJ/kg·K)	Specific exergy (kJ/kg) **
1	CO_2	203.00	194.50	2.400	603.67	2.0635	286.38
2	CO_2	135.84	92.80	2.400	557.96	2.0795	236.22
3	CO_2	132.88	91.90	2.400	554.72	2.0731	234.76
4	CO_2	97.96	91.50	2.400	508.01	1.9534	221.35
5	CO_2	97.96	91.50	0.672	508.01	1.9534	221.35
6	CO_2	172.02	194.85	0.672	559.57	1.9674	269.01
7	CO_2	97.96	91.50	1.728	508.01	1.9534	221.35
8	CO_2	45.00	90.90	1.728	386.97	1.5963	199.63
9	CO_2	93.69	195.05	1.728	413.91	1.6043	224.34
10	CO_2	121.52	194.85	1.728	475.15	1.7656	240.73
11	CO_2	132.36	194.85	2.400	495.41	1.8162	246.90
12	CO_2	134.67	194.55	2.400	499.68	1.8269	248.19
13	water	20.00	3.00	4.322	84.19	0.2964	1.84
14	water	31.00	2.90	4.322	130.17	0.4504	4.98
15	combustion gasses	232.00	1.15	3.140	634.69	4.3791	73.30
16	combustion gasses	150.25	1.03	3.140	551.02	4.2301	31.07

** O. P. = Operating Point (in accordance with Figure 1)*
*** At ambient temperature of 5 °C and ambient pressure of 1 bar*

5. Exergy analysis and the ambient temperature variation results of the CO_2 low-power marine waste heat recovery plant and its components at various loads

Figure 2 illustrates the mechanical power produced by the turbine, the mechanical power consumed by the main and auxiliary compressors, and the useful mechanical power at the three plant loads analyzed. Under all operating conditions, the turbine must generate at least sufficient mechanical power to drive both compressors (in which case the useful mechanical power would be zero). In real operating conditions at all loads, the turbine produces more mechanical power than required by the compressors, resulting in positive useful mechanical power, which is used to drive the electrical generator (Figure 1).

At the highest observed plant load (LOAD 100%), both produced and consumed mechanical power reach their maximum value, as does the useful mechanical power. A decrease in plant load results in a simultaneous reduction in turbine power output, compressor power consumption, and useful mechanical power (Figure 2).

As previously noted, the analyzed plant is classified as a low-power plant because at nominal load (LOAD 100%) it generates only 146.95 kW of useful power. At partial loads (LOAD 45% and LOAD 20%), the useful mechanical power amounts to 64.39 kW and 28.50 kW, respectively.

The plant utilizes waste heat in the form of combustion gases from a marine internal combustion engine. Without this plant, the waste heat from combustion gases would be discharged into the atmosphere and entirely lost. Therefore, regardless of the absolute level of useful mechanical power produced, the plant contributes to effective waste heat utilization.

The useful mechanical power of the plant can be increased in many different ways and through various plant modifications. However, the most influential parameters affecting useful power output are the heat flow and temperature of combustion gases. An increase in combustion gas heat flow and temperature would result in higher useful power generation. Nevertheless, such improvements are beneficial only up to a certain optimal level. Beyond this optimum, substantial system modifications and the addition of new components would be required to ensure proper utilization of the increased thermal input. Determining this optimal operating level represents an important direction for future research related to the analyzed plant.

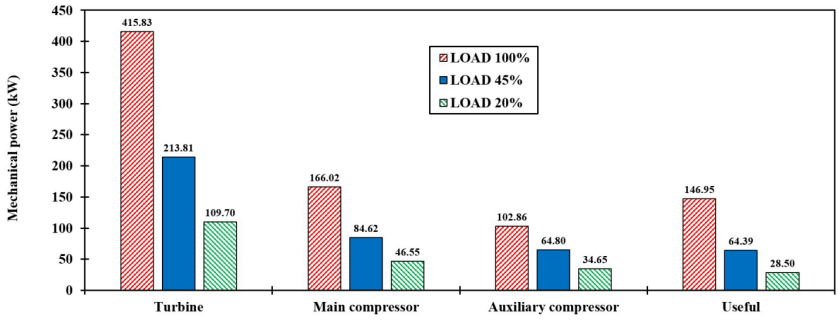

Figure 2. Produced (turbine), consumed (main and auxiliary compressor) and useful mechanical power in the power plant at three observed loads

The exergy efficiencies of the turbine, main compressor, and auxiliary compressor under varying ambient temperatures at all three observed plant loads are presented in Figure 3. As shown in Figure 3, the ambient temperature varies from 5 °C up to 40 °C in increments of 5 °C for each component and load condition.

Several important observations can be drawn from Figure 3. First, an increase in ambient temperature results in a decrease in the exergy efficiency of the turbine, main and auxiliary compressor at all observed plant loads. Previous studies [42, 51] have reported that higher ambient temperatures lead to increased exergy destruction and reduced exergy efficiency of various turbomachines, which is consistent with the results presented in Figure 3. However, for all turbomachines mentioned, the variation in exergy efficiency between 5 °C and 40 °C is relatively small at each plant load.

At all analyzed plant loads and ambient temperatures, the auxiliary compressor exhibits higher exergy efficiencies than both the main compressor and the turbine. At nominal load (LOAD 100%), the turbine shows higher exergy efficiency than the main compressor. In contrast, at partial loads (LOAD 45% and LOAD 20%) the main compressor achieves slightly higher exergy efficiencies than the turbine (Figure 3).

Overall, the turbomachines demonstrate satisfactory performance. Even at the highest ambient temperature considered (40 °C) and under all load conditions, the exergy efficiency of each turbomachine remains above 90%.

The exergy efficiencies of the high-temperature recuperator, low-temperature recuperator, and main heater under varying ambient temperature at all three observed plant loads are presented in Figure 4. For these three components at each load, the ambient temperature varies from 5 °C up to 40 °C in increments of 5 °C.

As for all turbomachines, and for both recuperators and the main heater, it can be concluded that an increase in the ambient temperature leads to higher exergy destruction and consequently lower exergy efficiencies.

At all observed loads and ambient temperatures, the low-temperature recuperator exhibits the highest exergy efficiencies, followed by the high-temperature recuperator,

while the main heater shows the lowest exergy efficiency among these components. Minor deviations from this trend occur at the lowest observed ambient temperatures and partial loads (LOAD 45% and LOAD 20%), where the high-temperature recuperator achieves slightly higher exergy efficiency than the low-temperature recuperator.

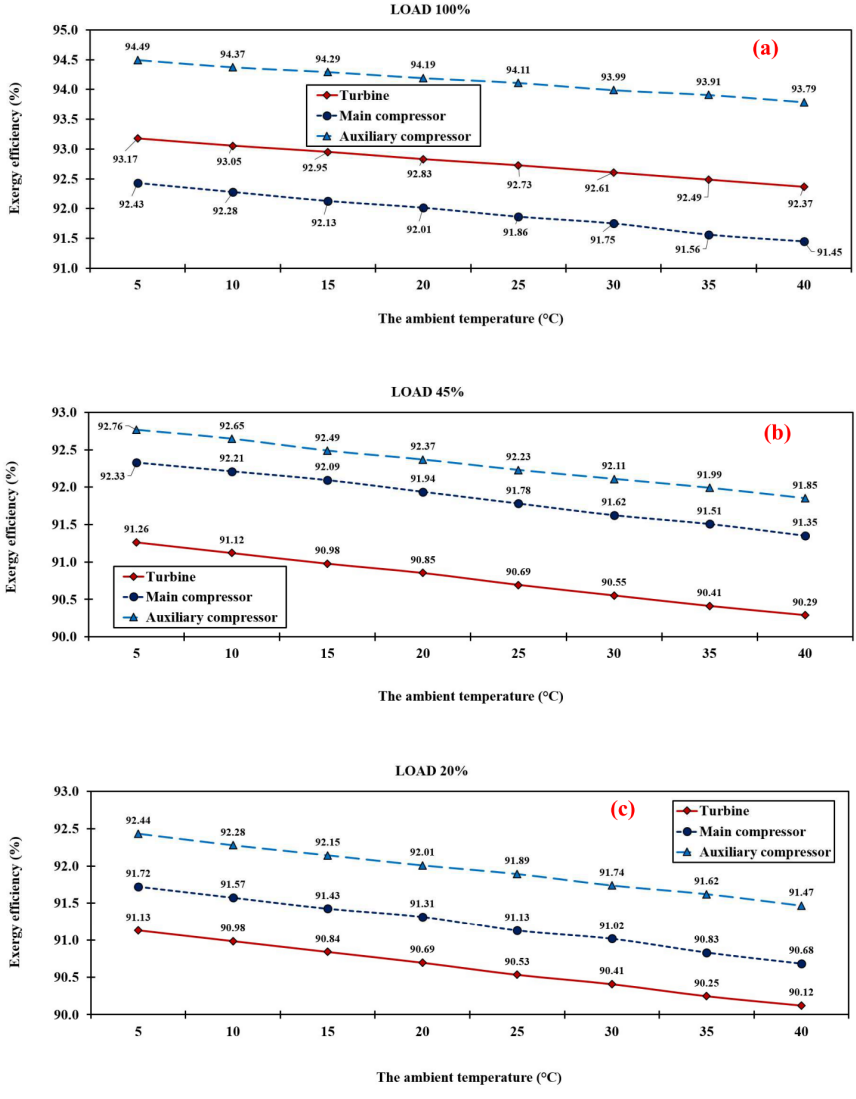

Figure 3. Turbomachines exergy efficiency (turbine, main and auxiliary compressor) during the ambient temperature variation at: (a) LOAD 100%, (b) LOAD 45%, and (c) LOAD 20%

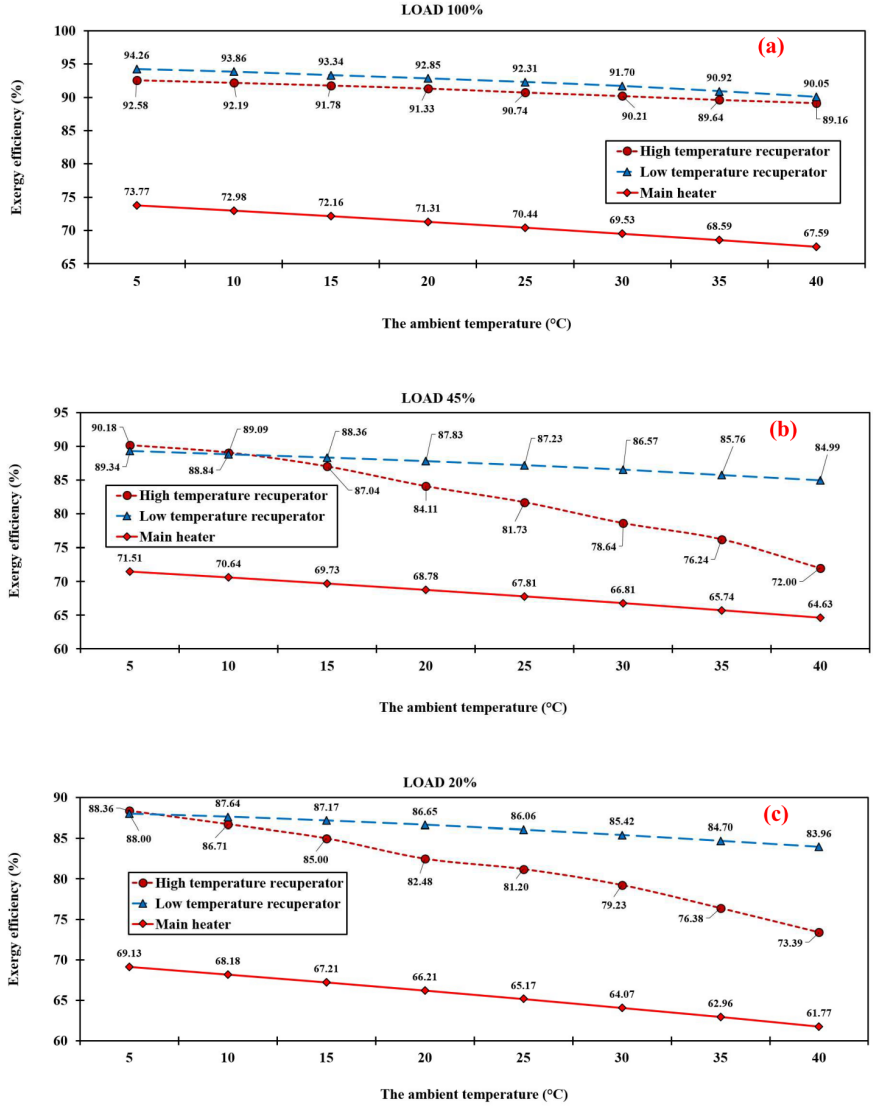

Figure 4. Exergy efficiency of high- and low-temperature recuperator, as well as the main heater during the ambient temperature variation at: (a) LOAD 100%, (b) LOAD 45%, and (c) LOAD 20%

Considering all loads and ambient temperatures, the exergy efficiency of the low-temperature recuperator ranges from 83.96% to 94.26%, that of the high-temperature

recuperator from 72.00% to 92.58%, and that of the main heater from 61.77% to 73.77% (Figure 4). For both recuperators and the main heater, these values can be regarded as reasonable and expected.

Figure 4 also shows an interesting phenomenon related to the high-temperature recuperator at partial loads. At both partial loads (LOAD 45% and LOAD 20%), an increase in ambient temperature leads to a significantly greater decrease in the exergy efficiency of the high-temperature recuperator compared to nominal load (LOAD 100%) and also compared to the low-temperature recuperator and the main heater. The reason for such occurrence is the fact that at both partial loads temperature and specific exergy differences between inlet and outlet CO_2 flow streams related to the high-temperature recuperator become very small, which results in high ambient temperature change sensitivity. The differences mentioned are not so small at nominal load, so at nominal load high-temperature recuperator is not highly influenced by ambient temperature variations.

For all six previously analyzed components from the power plant (turbine, main and auxiliary compressor, high- and low-temperature recuperator, and main heater) at all observed loads, the ambient temperature varied between 5 °C and 40 °C. In all cases, an increase in ambient temperature resulted in a decrease in exergy efficiency. However, the magnitude of exergy efficiency change differs among components. Therefore, the cumulative reduction in exergy efficiency during the ambient temperature increase from 5 °C to 40 °C for all six components is presented in Figure 5 for each load.

Figure 5 clearly indicates that the exergy efficiencies of all turbomachines (turbine, main and auxiliary compressor) are significantly less affected by ambient temperature variation than those of the heat exchangers (including the cooler, which is the most sensitive heat exchanger to ambient temperature changes, as shown in Figure 6). Within the analyzed ambient temperature range, the cumulative exergy efficiency change of each turbomachine at any load is approximately 1% or less.

In contrast, for the high- and low-temperature recuperators, and the main heater, the cumulative exergy efficiency change of each heat exchanger within the same ambient temperature range is approximately 4% or greater at all loads. At nominal load, the high-temperature recuperator is less sensitive to ambient temperature changes than the main heater and low-temperature recuperator. However, at partial loads (LOAD 45% and LOAD 20%), the opposite trend is observed due to the reduced temperature and specific exergy differences between inlet and outlet CO_2 flow streams in the high-temperature recuperator (Figure 5).

This analysis confirms that turbomachines are considerably less influenced by ambient temperature variations than heat exchangers.

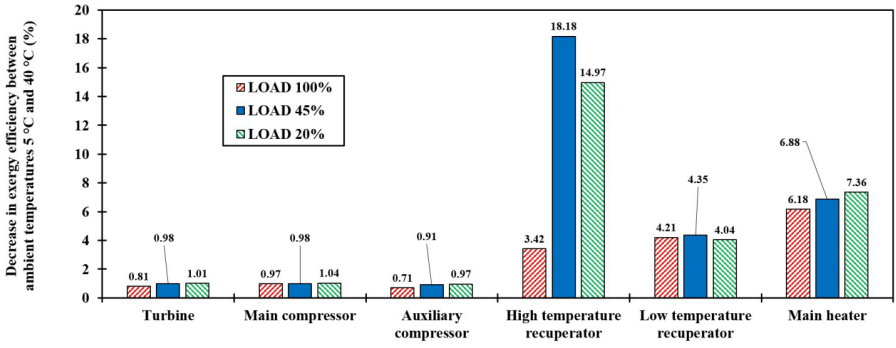

Figure 5. Decrease in exergy efficiency between ambient temperatures 5 °C and 40 °C for all turbomachines, high- and low-temperature recuperator, and main heater at three observed loads

Within the analyzed plant, the cooler is treated separately because the ambient temperature variation for this component cannot be performed over the same range as for other plant components. For the cooler, the ambient temperature varies from 5 °C to 25 °C in increments of 5 °C. The reason for this restricted range is evident in Figure 6 (a): at an ambient temperature of 30 °C, the cooler exergy efficiency becomes negative. This indicates that, under the operating parameters specified in Tables 4-6, the cooler cannot operate properly at ambient temperature of 30 °C or higher.

Figure 6 (a) also shows that the cooler exhibits the lowest exergy efficiencies among all components of the analyzed waste heat recovery plant, at all considered loads and ambient temperatures. Even at the lowest ambient temperature of 5 °C, the cooler exergy efficiency does not exceed 38%, which is relatively low for a heat exchanger. Furthermore, Figures 6(a) and 6(b) demonstrate that an increase in ambient temperature causes a substantial reduction in cooler exergy efficiency. An increase in ambient temperature from 5 °C to 25 °C results in a cumulative decrease in cooler exergy efficiency of approximately 35% or more at all loads. Such a pronounced exergy efficiency change within a relatively low ambient temperature range is not observed for any other plant component.

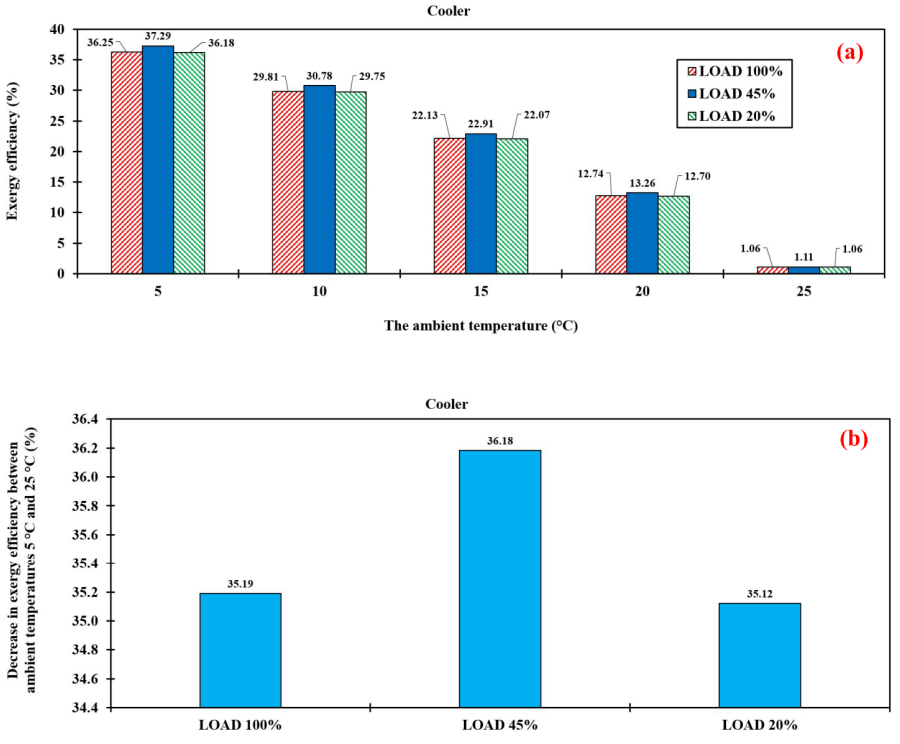

Figure 6. Cooler exergy efficiency at three observed power plant loads: (a) During the ambient temperature variation and (b) Decrease between ambient temperatures 5 °C and 25 °C

The reasons for the low exergy efficiency and high the ambient temperature sensitivity of the cooler can be identified from Tables 4-6 and are associated with the specific exergy of the cooling water. As shown in these tables (operating points 13 and 14), the difference in specific exergy between the cooler outlet and inlet are very small (as well as the values of these specific exergies because cooling water is a fluid whose operating parameters are very close to the ambient conditions). For the cooler, the difference in cooling water specific exergy (between outlet and inlet) multiplied by the water mass flow rate represents exergy outlet (Eq. 30). As the cooler exergy outlet is the numerator in the cooler exergy efficiency equation (Eq. 38), small numeric values in the numerator result in low cooler exergy efficiency and simultaneously in high cooler sensitivity to the ambient temperature change.

Figure 7 presents the exergy efficiency of the entire analyzed power plant at three loads and during ambient temperature variation (from 5 °C up to 40 °C in increments of 5 °C).

As observed for individual components, the overall plant exergy efficiency decreases with increasing ambient temperature at all loads. Figure 7(a) also clearly indicates that plant exergy efficiency decreases as load decreases, regardless of ambient temperature. Over the analyzed ambient temperature range, the exergy efficiency of the whole plant at nominal load (LOAD 100%) varies between 32.42% and 34.10%, at LOAD 45% exergy efficiencies of the whole plant varies from 27.06% to 28.66%, while at the lowest load (LOAD 20%) exergy efficiencies of the whole plant vary between 22.64% and 23.95%. Therefore, under the most favourable operating conditions, the exergy efficiency of the whole plant reaches approximately 34%. This relatively low exergy efficiency of the whole plant can be attributed to the fact that the plant utilizes only a single waste heat flow in the main heater from marine low-speed diesel engine (that heat flow is combustion gases). For closed-cycle gas turbine CO_2 waste heat recovery plants, it is advisable to exploit multiple waste heat flows from the internal combustion engine at different temperature levels. Such an approach can significantly increase the overall exergy efficiency of the whole plant. For example, [69] describes a similar CO_2 marine waste heat recovery plant which utilizes three waste heat flows from the internal combustion engine at three temperature levels – that waste heat flows are cooling water at the engine outlet, warm compressed air (after charger), and combustion gases at the engine outlet. Mentioned marine plant which uses three different waste heat flows from the internal combustion engine at three temperature levels can reach exergy efficiency of around 51% [69].

The analyzed CO_2 waste heat recovery plant is most sensitive to ambient temperature variations at nominal load (LOAD 100%) and this sensitivity decreases as the load decreases (Figure 7(b)). Between ambient temperatures of 5 °C and 40 °C, the cumulative change in overall plant exergy efficiency is 1.68 % at LOAD 100%, 1.60% at LOAD 45%, and only 1.32% at LOAD 20%.

For the plant analyzed in this paper, the preferable operating regime is nominal load (LOAD 100%). At nominal load, the plant generates the highest useful power (146.95 kW) and achieves the highest exergy efficiency (higher than 30%), regardless of the observed ambient temperature. However, it must be highlighted that at nominal load, the exergy efficiency of the whole CO_2 waste heat recovery plant is also the most sensitive to ambient temperature variations, which is particularly relevant in operating conditions where frequent ambient temperature fluctuations occur.

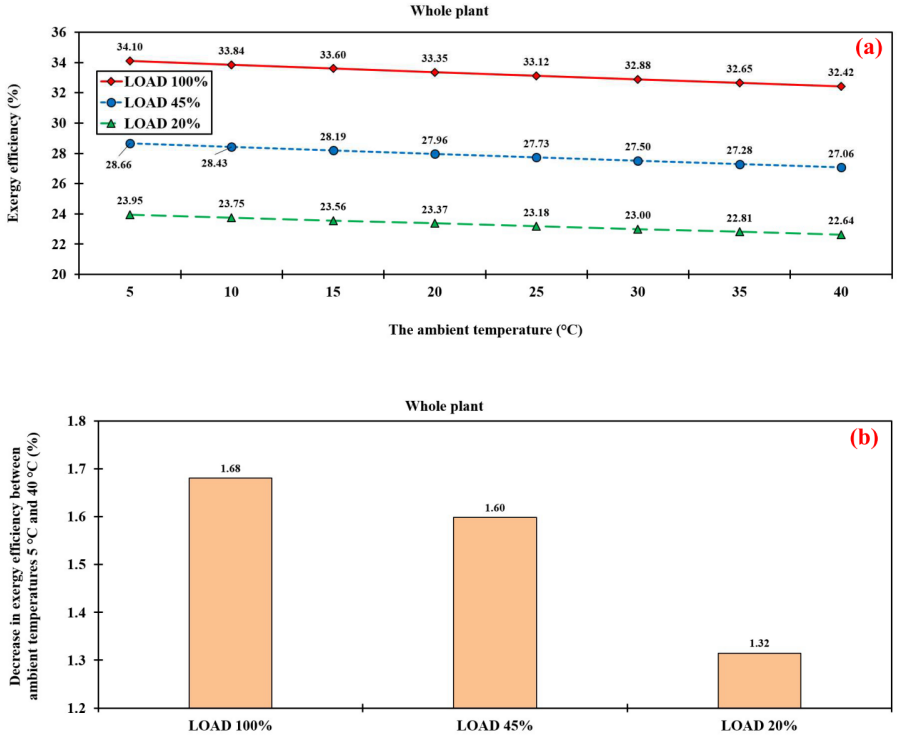

Figure 7. Whole plant exergy efficiency at three observed loads: (a) During the ambient temperature variation and (b) Decrease between ambient temperatures 5 °C and 40 °C

6. Conclusions

This paper presents exergy analysis, and the ambient temperature variation of marine CO_2 closed-cycle gas turbine low-power waste heat recovery plant. Waste heat recovery plant is analyzed from an exergy perspective, and the ambient temperature variation is performed under three different load conditions. The analysis and ambient temperature variation is evaluated for both individual components and the overall plant. The most significant conclusions obtained in this research are summarized as follows:

The analyzed waste heat recovery plant is classified as a low-power plant because at nominal load (LOAD 100%) it produces 146.95 kW of useful power, while at partial loads (LOAD 45% and LOAD 20%) the useful mechanical power produced by this plant is 64.39 kW and 28.50 kW, respectively.

An increase in ambient temperature leads to higher exergy destruction and a simultaneous decrease in exergy efficiency for both the overall plant and each plant component.

Considering all loads and ambient temperatures, all turbomachines from the analyzed plant (turbine, main compressor, and auxiliary compressor) exhibit high exergy efficiencies exceeding 90%. In general, the exergy efficiencies of the turbomachines are higher than those of the heat exchanger from the observed power plant.

Considering all loads and ambient temperatures, the exergy efficiencies of the low-temperature recuperator ranges from 83.96% to 94.26%, that of the high-temperature recuperator from 72.00% to 92.58%, while the exergy efficiencies of the main heater range from 61.77% to 73.77%.

At both partial loads (LOAD 45% and LOAD 20%), an increase in the ambient temperature notably decreases the high-temperature recuperator exergy efficiency, much higher than at the nominal load (LOAD 100%) and that of the low-temperature recuperator and the main heater.

Within the analyzed ambient temperature range, the cumulative change in exergy efficiency of each turbomachine at any load is approximately 1% or less, while the cumulative change in exergy efficiency for each heat exchanger at any load is approximately 4% or greater. Therefore, turbomachines are significantly less affected by ambient temperature variations than heat exchangers.

The cooler exhibits the lowest exergy efficiency among all plant components at all loads and ambient temperatures, with values not exceeding 38%. Moreover, its exergy efficiency is several times more sensitive to ambient temperature variations than that of any other plant component.

Under the most favorable operating conditions, the overall plant exergy efficiency reaches approximately 34%. This relatively low exergy efficiency can be attributed to the use of only a single waste heat flow from a marine low-speed diesel engine (combustion gases). For CO_2 waste heat recovery plants, the utilization of multiple waste heat streams from the internal combustion engine at different temperature levels is recommended, as this approach can significantly increase overall plant exergy efficiency.

The entire CO_2 waste heat recovery plant is most sensitive to ambient temperature variations at nominal load (LOAD 100%), and this sensitivity decreases as load decreases.

Future research related to the analyzed plant will focus on investigating various improvement strategies, both with and without structural modifications. Further optimization studies are also required. Finally, given that this is a low-power plant, the possibilities and limitations in increasing its useful power output should be analyzed.

Acknowledgment

This work was supported by the Croatian Science Foundation under the project number HRZZ-IP-2022-10-2821; University of Rijeka scientific grants uniri-iz-25-6, uniri-iz-25-220 and uniri-iz-25-10 (Funded by the European Union – NextGenerationEU); SPIN projects IP.1.1.03.0120, IP.1.1.03.0028 and IP.1.1.03.0039; University North project UNIN-TEH-25-1-8; the EU NextGeneration under the Juraj Dobrila University of Pula institutional research project number IIP_010144 and IIP_010136; and the EC Digital Europe Programme EDIH Adria 101083838.

References

1. Dere, C., & Deniz, C. (2020). Effect analysis on energy efficiency enhancement of controlled cylinder liner temperatures in marine diesel engines with model based approach. Energy Conversion and Management, 220, 113015. (doi:10.1016/j.enconman.2020.113015)
2. Bilousov, I., Bulgakov, M., & Savchuk, V. (2020). *Modern Marine Internal Combustion Engines*. Springer International Publishing.
3. Lamas, M. I., de Dios Rodríguez, J., Castro-Santos, L., & Carral, L. M. (2019). Effect of multiple injection strategies on emissions and performance in the Wärtsilä 6L 46 marine engine. A numerical approach. *Journal of Cleaner Production*, 206, 1-10. (doi:10.1016/j.jclepro.2018.09.165)
4. Tadros, M., Ventura, M., & Soares, C. G. (2019). Optimization procedure to minimize fuel consumption of a four-stroke marine turbocharged diesel engine. *Energy*, 168, 897-908. (doi:10.1016/j.energy.2018.11.146)
5. Agarwal, A. K., Kumar, D., Sharma, N., & Sonawane, U. (2022). *Engine Modeling and Simulation*. Springer Singapore.
6. Senčić, T., Mrzljak, V., Medica-Viola, V., & Wolf, I. (2022). CFD Analysis of a Large Marine Engine Scavenging Process. *Processes*, 10(1), 141. (doi:10.3390/pr10010141)
7. Liu, L., Wu, Y., & Wang, Y. (2022). Numerical investigation on knock characteristics and mechanism of large-bore natural gas dual-fuel marine engine. *Fuel*, 310, 122298. (doi:10.1016/j.fuel.2021.122298)
8. Muše, A., Jurić, Z., Račić, N., & Radica, G. (2020). Modelling, performance improvement and emission reduction of large two-stroke diesel engine using multi-zone combustion model. *Journal of Thermal Analysis and Calorimetry*, 1-14. (doi:10.1007/s10973-020-09321-7)
9. Okubo, M., & Kuwahara, T. (2019). *New technologies for emission control in marine diesel engines*. Butterworth-Heinemann.
10. Long, Y., Li, G., Zhang, Z., & Liang, J. (2021). Application of reformed exhaust gas recirculation on marine LNG engines for NOx emission control. *Fuel*, 291, 120114. (doi:10.1016/j.fuel.2020.120114)
11. Senčić, T., Mrzljak, V., Blecich, P., & Bonefačić, I. (2019). 2D CFD simulation of water injection strategies in a large marine engine. *Journal of Marine Science and Engineering*, 7(9), 296. (doi:10.3390/jmse7090296)
12. Lamas Galdo, M. I., Castro-Santos, L., & Rodriguez Vidal, C. G. (2020). Numerical analysis of NOx reduction using ammonia injection and comparison with water injection. *Journal of Marine Science and Engineering*, 8(2), 109. (doi:10.3390/jmse8020109)
13. Lu, Z., Lu, T., Shi, L., Wang, T., Wang, H., & Liu, M. (2022). An efficient approach to improve thermal efficiency on a low-speed two-stroke marine diesel engine. *Fuel*, 329, 125386. (doi:10.1016/j.fuel.2022.125386)
14. Yu, H., Wang, W., Sheng, D., Li, H., & Duan, S. (2022). Performance of combustion process on marine low speed two-stroke dual fuel engine at different fuel conditions: Full diesel/diesel ignited natural gas. *Fuel*, 310, 122370. (doi:10.1016/j.fuel.2021.122370)

15. Liu, X., Nguyen, M. Q., Chu, J., Lan, T., & He, M. (2020). A novel waste heat recovery system combing steam Rankine cycle and organic Rankine cycle for marine engine. *Journal of Cleaner Production*, 265, 121502. (doi:10.1016/j.jclepro.2020.121502)
16. Singh, D. V., & Pedersen, E. (2016). A review of waste heat recovery technologies for maritime applications. *Energy conversion and management*, 111, 315-328. (doi:10.1016/j.enconman.2015.12.073)
17. Sakalis, G. (2021). Investigation of supercritical CO2 cycles potential for marine Diesel engine waste heat recovery applications. *Applied Thermal Engineering*, 195, 117201. (doi:10.1016/j.applthermaleng.2021.117201)
18. Díaz-Secades, L. A., González, R., Rivera, N., Montañés, E., & Quevedo, J. R. (2023). Waste heat recovery system for marine engines optimized through a preference learning rank function embedded into a Bayesian optimizer. *Ocean Engineering*, 281, 114747. (doi:10.1016/j.oceaneng.2023.114747)
19. Lion, S., Vlaskos, I., & Taccani, R. (2020). A review of emissions reduction technologies for low and medium speed marine Diesel engines and their potential for waste heat recovery. *Energy Conversion and Management*, 207, 112553. (doi:10.1016/j.enconman.2020.112553)
20. Qu, J., Feng, Y., Zhu, Y., Zhou, S., & Zhang, W. (2021). Design and thermodynamic analysis of a combined system including steam Rankine cycle, organic Rankine cycle, and power turbine for marine low-speed diesel engine waste heat recovery. *Energy Conversion and Management*, 245, 114580. (doi:10.1016/j.enconman.2021.114580)
21. Kallis, G., Roumpedakis, T. C., Pallis, P., Koutantzi, Z., Charalampidis, A., & Karellas, S. (2022). Life cycle analysis of a waste heat recovery for marine engines Organic Rankine Cycle. *Energy*, 257, 124698. (doi:10.1016/j.energy.2022.124698)
22. Mohammed, A. G., Mosleh, M., El-Maghlany, W. M., & Ammar, N. R. (2020). Performance analysis of supercritical ORC utilizing marine diesel engine waste heat recovery. *Alexandria Engineering Journal*, 59(2), 893-904. (doi:10.1016/j.aej.2020.03.021)
23. Pan, P., Yuan, C., Sun, Y., Yan, X., Lu, M., & Bucknall, R. (2020). Thermo-economic analysis and multi-objective optimization of S-CO2 Brayton cycle waste heat recovery system for an ocean-going 9000 TEU container ship. *Energy Conversion and Management*, 221, 113077. (doi:10.1016/j.enconman.2020.113077)
24. Mrzljak, V., Poljak, I., Prpić-Oršić, J., & Jelić, M. (2020). Exergy analysis of marine waste heat recovery CO2 closed-cycle gas turbine system. *Pomorstvo*, 34(2), 309-322. (doi:10.31217/p.34.2.12)
25. Hou, S., Wu, Y., Zhou, Y., & Yu, L. (2017). Performance analysis of the combined supercritical CO2 recompression and regenerative cycle used in waste heat recovery of marine gas turbine. *Energy Conversion and Management*, 151, 73-85. (doi:10.1016/j.enconman.2017.08.082)
26. Kostyuk, A., & Frolov, V. (1988). *Steam and gas turbines*. Mir Publishers.
27. Giampaolo, T. (2020). *Gas turbine handbook: principles and practice*. River Publishers. (doi:10.1201/9781003151821)
28. Badran, O. O. (1999). Gas-turbine performance improvements. *Applied Energy*, 64(1-4), 263-273. (doi:10.1016/S0306-2619(99)00088-4)
29. Mrzljak, V., Perčić, G., & Prpić-Oršić, J. (2018). Gas turbine upgrade with heat regenerator-numerical analysis of advantages and disadvantages. In *III International Scientific Conference: Industry 4.0* (pp. 184-187).
30. Tejedor, T. Á. (2011). Gas turbine materials selection, life management and performance improvement. Power plant life management and performance improvement, 330-419. (doi:10.1533/9780857093806.3.330)
31. Xie, L., & Yang, J. (2022). Performance Modulation of S-CO2 Brayton Cycle for Marine Low-Speed Diesel Engine Flue Gas Waste Heat Recovery Based on MOGA. *Entropy*, 24(11), 1544. (doi:10.3390/e24111544)
32. Sekulic, D. P., & Shah, R. K. (2023). *Fundamentals of heat exchanger design*. John Wiley & Sons.
33. Anđelić, N., Baressi Šegota, S., Lorencin, I., Poljak, I., Mrzljak, V., & Car, Z. (2021). Use of Genetic Programming for the Estimation of CODLAG Propulsion System Parameters. *Journal of Marine Science and Engineering*, 9(6), 612. (doi:10.3390/jmse9060612)
34. Baressi Šegota, S., Mrzljak, V., Anđelić, N., Poljak, I., & Car, Z. (2023). Use of Synthetic Data in Maritime Applications for the Problem of Steam Turbine Exergy Analysis. *Journal of marine science and engineering*, 11(8), 1595. (doi:10.3390/jmse11081595)

35. Anđelić, N., Šegota, S. B., & Mrzljak, V. (2025). A comprehensive study on symbolic expressions for fault detection-classification in photovoltaic farms. *Applied energy*, 383, 125370. (doi:10.1016/j.apenergy.2025.125370)
36. Mrzljak, V., Kudláček, J., Baressi Šegota, S., & Medica-Viola, V. (2021). Energy and Exergy Analysis of Waste Heat Recovery Closed-Cycle Gas Turbine System while Operating with Different Medium. *Pomorski zbornik*, 60(1), 21-48. (doi:10.18048/2021.60.02)
37. Dincer, I., & Rosen, M. A. (2012). *Exergy: energy, environment and sustainable development*. Newnes.
38. Poljak, I., Mrzljak, V., Senčić, T., & Pastorčić, D. (2024). Isentropic and exergy analyses of marine steam turbine segments at several loads. Scientific Journal of Maritime Research-*Pomorstvo*, 38(1). (doi:10.31217/p.38.1.8)
39. Kanoğlu, M., Çengel, Y. A. & Dincer, I. (2012). Efficiency Evaluation of Energy Systems. *Springer Briefs in Energy*. (doi:10.1007/978-1-4614-2242-6)
40. Khaleel, O. J., Ismail, F. B., Ibrahim, T. K., & bin Abu Hassan, S. H. (2022). Energy and exergy analysis of the steam power plants: A comprehensive review on the Classification, Development, Improvements, and configurations. *Ain Shams Engineering Journal*, 13(3), 101640. (doi:10.1016/j.asej.2021.11.009)
41. Mrzljak, V., Prpić-Oršić, J., Poljak, I., & Šegota, S. B. (2020). Exergy analysis of steam condenser at various loads during the ambient temperature change. *Machines. Technologies. Materials*., 14(1), 12-15.
42. Kopac, M., & Hilalci, A. (2007). Effect of ambient temperature on the efficiency of the regenerative and reheat Çatalağzı power plant in Turkey. *Applied Thermal Engineering*, 27(8-9), 1377-1385. (doi:10.1016/j.applthermaleng.2006.10.029)
43. Dincer, I., Midilli, A., & Kucuk, H. (Eds.). (2014). *Progress in exergy, energy, and the environment*. Springer. (doi:10.1007/978-3-319-04681-5)
44. Anđelić, N., Mrzljak, V., Lorencin, I., & Baressi Šegota, S. (2020). Comparison of exergy and various energy analysis methods for a main marine steam turbine at different loads. *Pomorski zbornik*, 59(1), 9-34. (doi:10.18048/2020.59.01)
45. Elhelw, M., & Al Dahma, K. S. (2019). Utilizing exergy analysis in studying the performance of steam power plant at two different operation mode. *Applied Thermal Engineering*, 150, 285-293. (doi:10.1016/j.applthermaleng.2019.01.003)
46. Mrzljak, V., Anđelić, N., Lorencin, I., & Sandi Baressi Šegota, S. (2021). The influence of various optimization algorithms on nuclear power plant steam turbine exergy efficiency and destruction. *Pomorstvo*, 35(1), 69-86. (doi:10.31217/p.35.1.8)
47. Nikam, K. C., Kumar, R., & Jilte, R. (2021). Economic and exergoeconomic investigation of 660 MW coal-fired power plant. *Journal of Thermal Analysis and Calorimetry*, 145(3), 1121-1135. (doi:10.1007/s10973-020-10213-z)
48. Hoseinzadeh, S., & Stephan Heyns, P. (2021). Advanced energy, exergy, and environmental (3E) analyses and optimization of a coal-fired 400 MW thermal power plant. *Journal of Energy Resources Technology*, 143(8). (doi:10.1115/1.4048982)
49. Shamoushaki, M., Fiaschi, D., Manfrida, G., & Talluri, L. (2022). Energy, exergy, economic and environmental (4E) analyses of a geothermal power plant with NCGs reinjection. *Energy*, 244, 122678. (doi:10.1016/j.energy.2021.122678)
50. Sun, L., Wang, D., & Xie, Y. (2021). Energy, exergy and exergoeconomic analysis of two supercritical CO2 cycles for waste heat recovery of gas turbine. *Applied thermal engineering*, 196, 117337. (doi:10.1016/j.applthermaleng.2021.117337)
51. Aljundi, I. H. (2009). Energy and exergy analysis of a steam power plant in Jordan. *Applied thermal engineering*, 29(2-3), 324-328. (doi:10.1016/j.applthermaleng.2008.02.029)
52. Koroglu, T., & Sogut, O. S. (2018). Conventional and advanced exergy analyses of a marine steam power plant. *Energy*, 163, 392-403. (doi:10.1016/j.energy.2018.08.119)
53. Poljak, I., & Mrzljak, V. (2023). Thermodynamic Analysis and Comparison of Two Marine Steam Propulsion Turbines. *NAŠE MORE: znanstveni časopis za more i pomorstvo*, 70(2), 88-102. (doi:10.17818/NM/2023/2.2)
54. Mrzljak, V., Jelić, M., Poljak, I., & Prpić-Oršić, J. (2023). Analysis and comparison of main steam turbines from four different thermal power plants. *Pomorstvo*, 37(1), 58-74. (doi:10.31217/p.37.1.6)

55. Tan, H., Shan, S., Nie, Y., & Zhao, Q. (2018). A new boil-off gas re-liquefaction system for LNG carriers based on dual mixed refrigerant cycle. *Cryogenics*, 92, 84-92. (doi:10.1016/j.cryogenics.2018.04.009)
56. Ahmadi, G. R., & Toghraie, D. (2016). Energy and exergy analysis of Montazeri steam power plant in Iran. *Renewable and Sustainable Energy Reviews*, 56, 454-463. (doi:10.1016/j.rser.2015.11.074)
57. Uysal, C., Kurt, H., & Kwak, H. Y. (2017). Exergetic and thermoeconomic analyses of a coal-fired power plant. *International Journal of Thermal Sciences*, 117, 106-120. (doi:10.1016/j.ijthermalsci.2017.03.010)
58. Hafdhi, F., Khir, T., Yahyia, A. B., & Brahim, A. B. (2015). Energetic and exergetic analysis of a steam turbine power plant in an existing phosphoric acid factory. *Energy Conversion and Management*, 106, 1230-1241. (doi:10.1016/j.enconman.2015.10.044)
59. Erdem, H. H., Akkaya, A. V., Cetin, B., Dagdas, A., Sevilgen, S. H., Sahin, B., ... & Atas, S. (2009). Comparative energetic and exergetic performance analyses for coal-fired thermal power plants in Turkey. *International Journal of Thermal Sciences*, 48(11), 2179-2186. (doi:10.1016/j.ijthermalsci.2009.03.007)
60. Mrzljak, V., Poljak, I., Jelić, M., & Prpić-Oršić, J. (2023). Thermodynamic Analysis and Improvement Potential of Helium Closed Cycle Gas Turbine Power Plant at Four Loads. *Energies*, 16(15), 5589. (doi:10.3390/en16155589)
61. Noroozian, A., Mohammadi, A., Bidi, M., & Ahmadi, M. H. (2017). Energy, exergy and economic analyses of a novel system to recover waste heat and water in steam power plants. *Energy conversion and management*, 144, 351-360. (doi:10.1016/j.enconman.2017.04.067)
62. Ray, T. K., Datta, A., Gupta, A., & Ganguly, R. (2010). Exergy-based performance analysis for proper O&M decisions in a steam power plant. *Energy Conversion and Management*, 51(6), 1333-1344. (doi:10.1016/j.enconman.2010.01.012)
63. Mrzljak, V., Poljak, I., & Prpić-Oršić, J. (2019). Exergy analysis of the main propulsion steam turbine from marine propulsion plant. *Brodogradnja: Teorija i praksa brodogradnje i pomorske tehnike*, 70(1), 59-77. (doi:10.21278/brod70105)
64. Poljak, I., Orović, J., Mrzljak, V., & Bernečić, D. (2020). Energy and exergy evaluation of a two-stage axial vapour compressor on the LNG carrier. *Entropy*, 22(1), 115. (doi:10.3390/e22010115)
65. Kumar, S., Kumar, D., Memon, R. A., Wassan, M. A., & Ali, M. S. (2018). Energy and exergy analysis of a coal fired power plant. *Mehran University Research Journal of Engineering & Technology*, 37(4), 611-624. (doi:10.22581/muet1982.1804.13)
66. Ibrahim, T. K., Basrawi, F., Awad, O. I., Abdullah, A. N., Najafi, G., Mamat, R., & Hagos, F. Y. (2017). Thermal performance of gas turbine power plant based on exergy analysis. *Applied thermal engineering*, 115, 977-985. (doi:10.1016/j.applthermaleng.2017.01.032)
67. Adibhatla, S., & Kaushik, S. C. (2014). Energy and exergy analysis of a super critical thermal power plant at various load conditions under constant and pure sliding pressure operation. *Applied thermal engineering*, 73(1), 51-65. (doi:10.1016/j.applthermaleng.2014.07.030)
68. Naserbegi, A., Aghaie, M., Minuchehr, A., & Alahyarizadeh, G. (2018). A novel exergy optimization of Bushehr nuclear power plant by gravitational search algorithm (GSA). *Energy*, 148, 373-385. (doi:10.1016/j.energy.2018.01.119)
69. Mrzljak, V., Jelić, M., Poljak, I., & Medica-Viola, V. (2023). Exergy analysis of supercritical CO2 system for marine diesel engine waste heat recovery application. *Pomorski zbornik*, 63(1), 39-62.
70. Lemmon, E. W., Huber, M. L., & McLinden, M. O. (2010). NIST Standard Reference Database 23, Reference Fluid Thermodynamic and Transport Properties (REFPROP), version 9.0, National Institute of Standards and Technology. R1234yf. fld file dated December, 22, 2010.
71. Si, N., Zhao, Z., Su, S., Han, P., Sun, Z., Xu, J., ... & Xiang, J. (2017). Exergy analysis of a 1000 MW double reheat ultra-supercritical power plant. *Energy Conversion and Management*, 147, 155-165. (doi:10.1016/j.enconman.2017.05.045)
72. Kaushik, S. C., Reddy, V. S., & Tyagi, S. K. (2011). Energy and exergy analyses of thermal power plants: A review. *Renewable and Sustainable energy reviews*, 15(4), 1857-1872. (doi:10.1016/j.rser.2010.12.007)